NASA TECHNICAL MEMORANDUM

NASA TM X-2382

NASA TM X-2382

EXPERIMENTAL INVESTIGATION OF A LOW REYNOLDS NUMBER PARTIAL-ADMISSION SINGLE-STAGE SUPERSONIC TURBINE

by Louis J. Goldman

Lewis Research Center
Cleveland, Ohio 44135

NATIONAL AERONAUTICS AND SPACE ADMINISTRATION • WASHINGTON, D. C. • OCTOBER 1971

1. Report No.	2. Government Accession No.	3. Recipient's Catalog No.
NASA TM X-2382		

4. Title and Subtitle	5. Report Date
EXPERIMENTAL INVESTIGATION OF A LOW REYNOLDS NUMBER PARTIAL-ADMISSION SINGLE-STAGE SUPERSONIC TURBINE	October 1971
	6. Performing Organization Code
7. Author(s)	8. Performing Organization Report No.
Louis J. Goldman	E-6380
	10. Work Unit No.
9. Performing Organization Name and Address	120-34
Lewis Research Center National Aeronautics and Space Administration Cleveland, Ohio 44135	11. Contract or Grant No.
	13. Type of Report and Period Covered
12. Sponsoring Agency Name and Address	Technical Memorandum
National Aeronautics and Space Administration Washington, D.C. 20546	14. Sponsoring Agency Code

15. Supplementary Notes

16. Abstract

Turbine performance characteristics were obtained for a single-stage partial-admission supersonic turbine operating at low Reynolds numbers. The turbine was tested over a range of pressure ratios from 20 to 150 and equivalent speeds from 20 to 100 percent of design.

17. Key Words (Suggested by Author(s))	18. Distribution Statement
Supersonic turbine Experimental performance	Unclassified - unlimited

19. Security Classif. (of this report)	20. Security Classif. (of this page)	21. No. of Pages	22. Price*
Unclassified	Unclassified	22	$3.00

* For sale by the National Technical Information Service, Springfield, Virginia 22151

EXPERIMENTAL INVESTIGATION OF A LOW REYNOLDS NUMBER PARTIAL-ADMISSION SINGLE-STAGE SUPERSONIC TURBINE

by Louis J. Goldman

Lewis Research Center

SUMMARY

Turbine performance characteristics were obtained for a single-stage partial-admission supersonic turbine operating at a Reynolds number of approximately 75×10^3. The turbine was tested over a range of pressure ratios from 20 to 150 and equivalent speeds from 20 to 100 percent of design. In addition, the performance of the stator operating alone was obtained.

Testing of the stator alone indicated good agreement with theory for the divergent section of the nozzle. On the straight section, however, expansion and shock wave formation resulted in the pressure deviating from the theoretically constant design value.

The equivalent turbine specific work at a design pressure ratio of 63 and equivalent design speed was 78.1×10^3 joules per kilogram (33.6 Btu/lb) at a static efficiency of 0.390. This efficiency is considerably lower than that predicted by boundary layer calculations, which do not take into consideration losses due to shock wave formation (as were found to occur in the nozzle exit section). The performance, however, is in reasonable agreement with previous experimental results.

Increasing the turbine pressure ratio above the design value resulted in only a small increase in specific work, indicating that the turbine was operating near limiting loading. The maximum turbine efficiency obtained at any given speed occurred at or near the design pressure ratio and dropped off rapidly at off-design pressure ratios.

INTRODUCTION

Interest in supersonic turbines arises from their possible use in turbopump and open-cycle auxiliary space power systems, where high-energy fluids are used and high pressure ratios are available. To obtain the highest practical efficiency for this type of turbine, proper design methods must be used.

The design of both the supersonic nozzle and rotor blades can be accomplished by using the method of characteristics as applied to the isentropic flow of a perfect gas. Computer programs for these designs are presented in references 1 and 2. Analytically, blade losses are accounted for by correcting the isentropic profiles for the boundary layer displacement thickness. Methods for accomplishing this are described in references 3 and 4.

In order to verify the losses predicted by the analytical methods, experimental data are required. Experimental results for single- and two-stage supersonic turbines operating at Reynolds numbers around 4×10^5 have been reported in references 5 to 7. For the low Reynolds number range encountered in some of the auxiliary space power systems of interest, little if any experimental data exists.

This report presents experimental performance characteristics for a single-stage partial-admission supersonic turbine operating at a Reynolds number of approximately 75×10^3. The turbine was tested over a range of pressure ratios from 20 to 150 and equivalent speeds from 20 to 100 percent of design. In addition to obtaining overall turbine performance, the stator was tested alone and the results are also presented.

TURBINE DESIGN

General Characteristics

The single-stage supersonic turbine was aerodynamically designed to operate using hydrogen-oxygen combustion products at a turbine inlet temperature of 1389 K (2500° R) and a mean blade speed of 731.5 meters per second (2400 ft/sec). The turbine was tested using room-temperature air. The equivalent design conditions were

Specific work, $\Delta h/\theta_{cr}$, J/kg (Btu/lb)	10.56×10^4 (45.44)
Mean blade speed, $U_m/\sqrt{\theta_{cr}}$, m/sec (ft/sec)	136.9 (449.0)
Mass flow, $w\sqrt{\theta_{cr}}\epsilon/\delta$, kg/sec (lb/sec)	0.00336 (0.00739)
Pressure ratio, p_0'/p_2	63.0

In the design procedure, a turbine efficiency level of 50 percent was determined from boundary layer calculations for the stator and rotor. It is realized that other factors such as shock wave formation and flow separation would, if they occurred, decrease the predicted efficiencies. These other factors were not considered in the determination of the design velocity diagrams and specific work.

The turbine had a mean diameter of 0.218 meter (8.6 in.) and a hub-tip radius ratio of 0.923. The arc of admission was 9.2 percent and the design air Reynolds number Re was approximately 75×10^3 based on blade height (see ref. 8). A sketch of the stator and rotor blade shapes together with the velocity diagram is shown in figure 1.

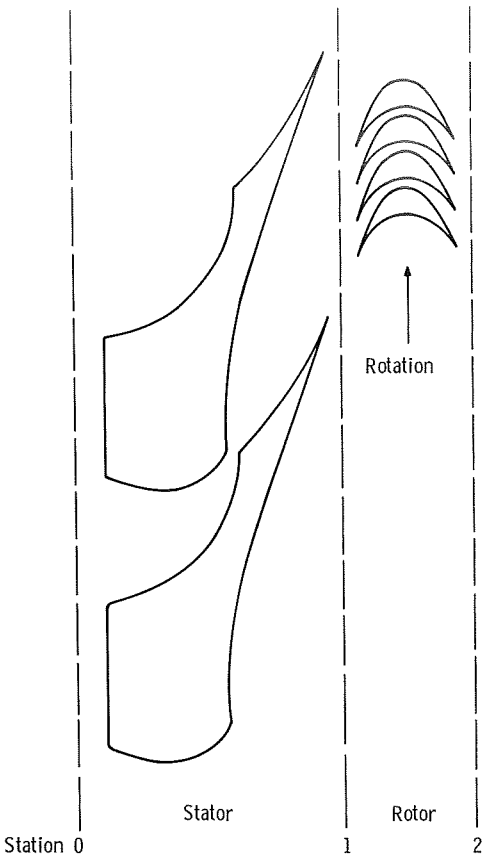

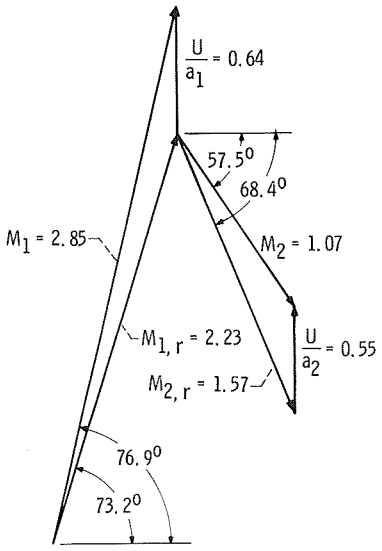

Figure 1. - Design velocity diagram.

Stator Design

The stator was designed with a sharp-edged throat so as to produce uniform parallel flow at the exit in the minimum possible distance. As seen in figure 2, the stator passage consisted of three sections: (1) a converging section, (2) a diverging section, and (3) a straight section on the suction surface. The converging section produced the flow turning with small losses. The diverging section accelerated the flow to the desired free-stream Mach number at the exit. The straight section on the suction surface completed the nozzle profile. The stator mean-section coordinates are given in table I.

The diverging section of the blade was designed by using the computer program described in reference 3. The program first calculated the isentropic nozzle profile for the given exit Mach number by using the method of characteristics. Boundary layer characteristics (momentum and displacement thicknesses) for the ideal nozzle were then obtained, and the nozzle profile was corrected to include the effect of the displacement thickness. The aftermixing conditions (Mach number, flow angle, pressure, etc.) were calculated by assuming that the flow mixes to uniform conditions downstream of the stators, as described in references 9 and 10.

The stator was designed for a free-stream Mach number before mixing of 3.65. The mixing calculations resulted in a 12.0 percent loss in kinetic energy and a 56.5 percent loss in total pressure. The aftermixing Mach number was 2.85. The stator consisted of two nozzles whose throat dimension was 0.112 centimeter (0.044 in.).

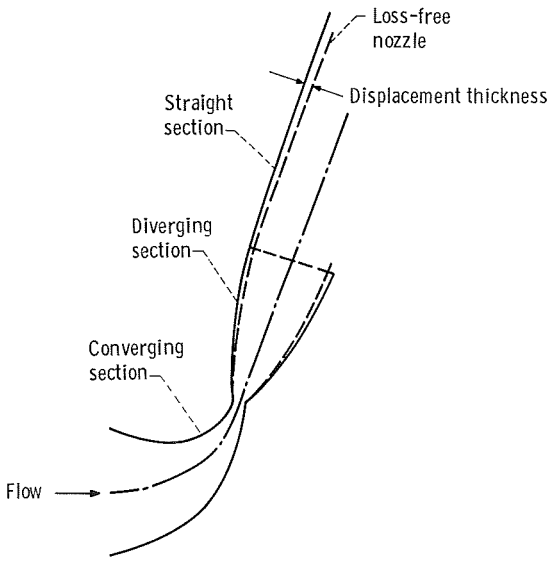

Figure 2. - Design of supersonic nozzle blade passage.

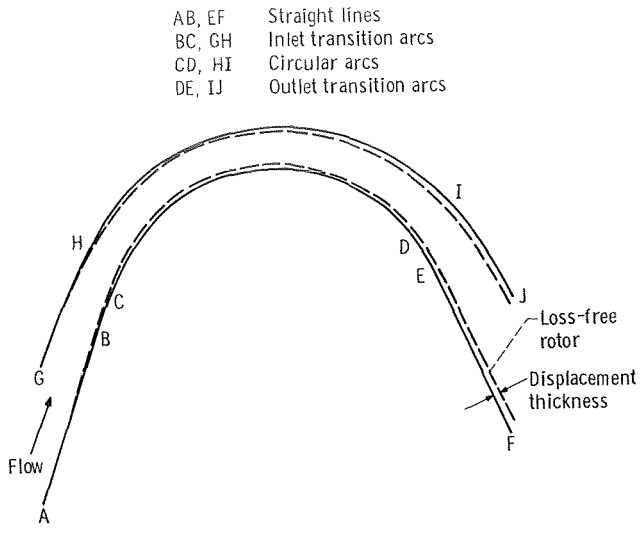

Figure 3. - Design of supersonic rotor blade passage.

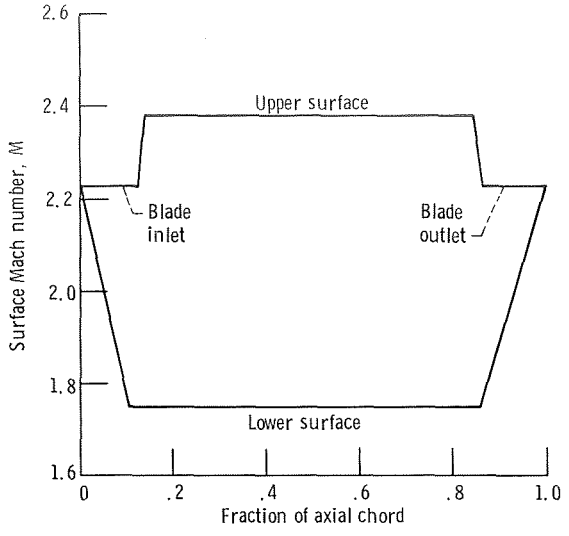

Figure 4. - Surface Mach number distribution for rotor blade.

Rotor Design

The design of the rotor was based on establishing vortex flow within the blade passage. The rotor passage, shown in figure 3, consisted essentially of three major parts: (1) inlet transition arcs, (2) circular arcs, and (3) outlet transition arcs. The inlet transition arcs (lower and upper) converted the uniform parallel flow at the passage inlet into vortex flow. The concentric circular arcs turned and maintained the vortex flow conditions. The outlet transition arcs reconverted the vortex flow into uniform parallel flow at the passage exit. Straight-line segments parallel to the inlet and outlet flow direction completed the passage. The rotor blade mean-section coordinates are given in table II.

The rotor blades were designed by using the procedure described in reference 4. The isentropic profile was first calculated by the method of characteristics for an outlet spacing less than the inlet spacing. Boundary layer parameters were then obtained and the rotor profile was corrected to include the effect of the displacement thickness. The aftermixing conditions were obtained as described previously. The rotor was designed for the surface Mach number distribution shown in figure 4. The rotor consisted of 170 blades whose solidity was 3.2.

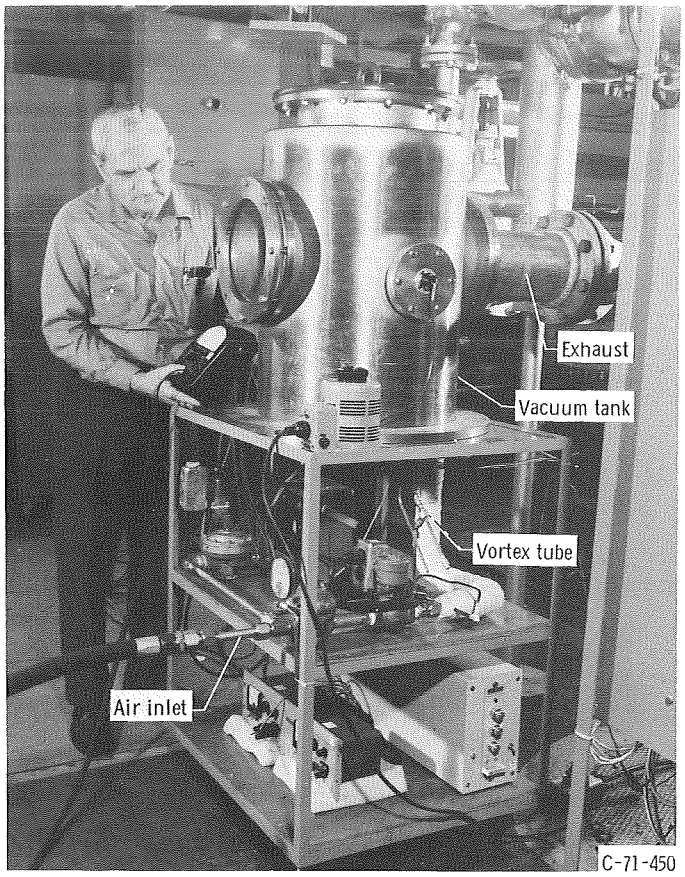

Figure 5. - Vacuum tank facility.

APPARATUS AND INSTRUMENTATION

Apparatus

The apparatus consisted of the single-stage turbine, a flywheel to absorb the power output of the turbine, and an inlet and outlet exhaust piping system. The experimental investigation was conducted in the vacuum tank shown in figure 5.

Pressurized air was used as the working fluid. The air, which was dried and filtered, passed through a pressure regulator before entering the stator. The stator was choked for all test conditions investigated and was flow calibrated prior to installation. After leaving the turbine, the air was exhausted into the laboratory low-pressure exhaust system. With a fixed exhaust pressure, the inlet pressure was remotely regulated to obtain the desired pressure ratio across the turbine.

A sketch of the turbine test assembly is shown in figure 6. The turbine shaft was vertical. The shaft was stationary and hollow to facilitate cooling of the bearings. The cooling air was provided by means of a vortex tube which converted compressed air into

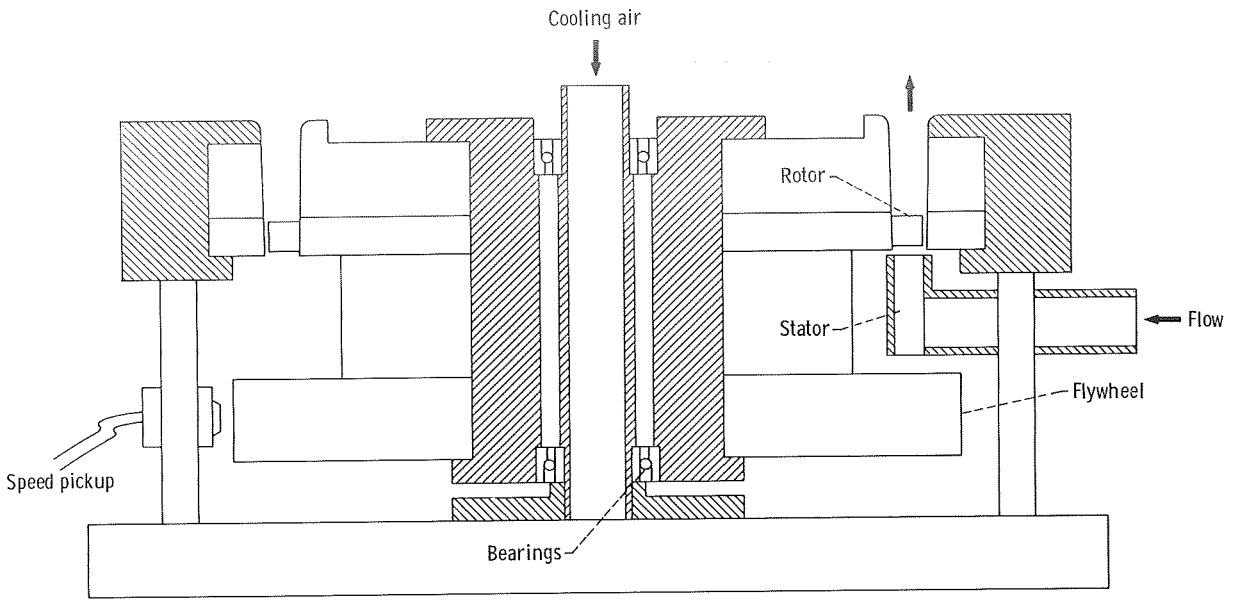

Figure 6. - Cross-sectional view of supersonic turbine.

Figure 7. - Turbine test assembly.

a cold and a hot airstream. Because of the vacuum environment, the bearings were solid lubricated. Standard bearings were modified by replacing the ball retainers with ones fabricated from a self-lubricating high-strength plastic material. The test assembly, stator, and rotor blade assemblies are shown in figures 7, 8, and 9, respectively.

Instrumentation

The turbine was instrumented so that overall turbine performance data could be obtained. Pressures were measured by using electronic transducers at the turbine inlet and in the vacuum tank. The turbine exhaust pressure was taken to be equal to the vacuum tank pressure. Temperatures were measured at the turbine inlet and on the bearing inner races. The rotational speed of the turbine was obtained by use of a Hall generator in conjunction with a small magnet embedded in the flywheel. Rotation of the flywheel caused the Hall crystal to generate series of pulses, whose frequency was proportional to the rotational speed of the turbine.

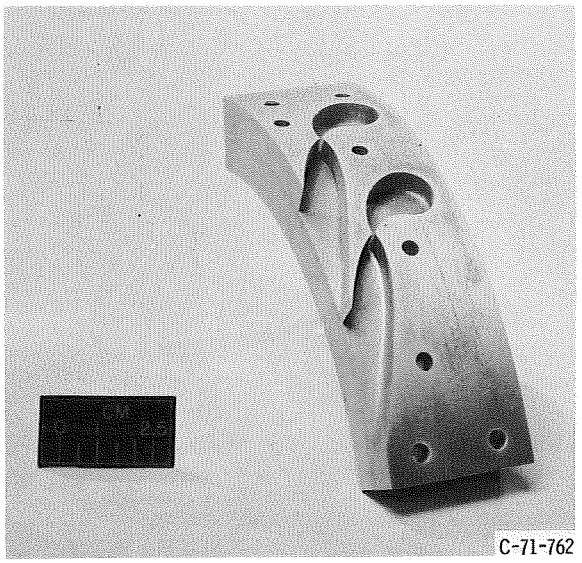

Figure 8. - Stator.

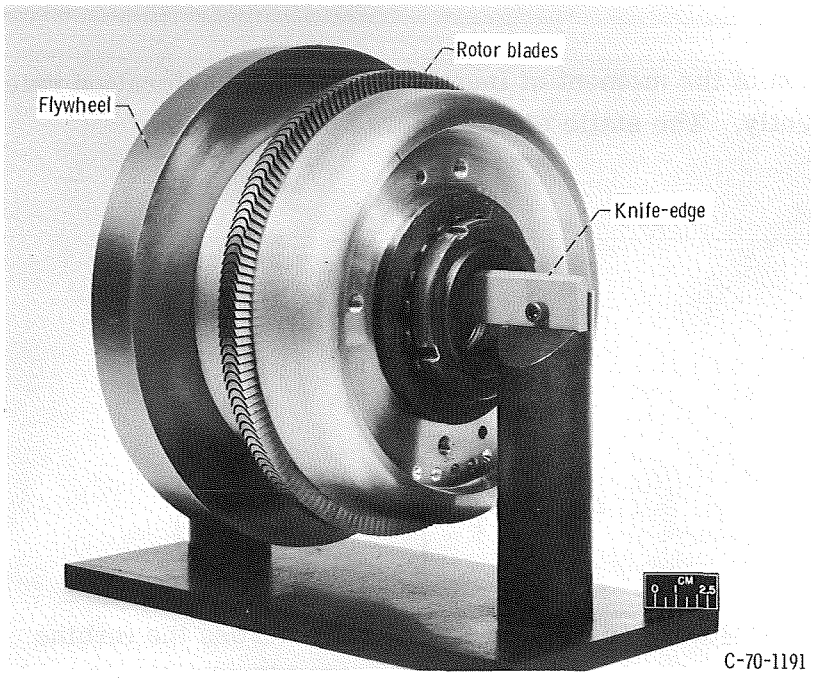

Figure 9. - Rotor.

PROCEDURE

The experimental tests were conducted by operating the turbine at constant pressure ratios. The turbine speed was allowed to vary from zero to slightly over equivalent design speed, at which point the airflow was shut off. Data were taken over a range of total- to static-pressure ratios from 20 to 150. The nominal exhaust pressure was 8300 newtons per square meter (173 lb/ft^2).

The equivalent specific work $\Delta h/\theta_{cr}$ of the turbine was calculated from the equation

$$\frac{\Delta h}{\theta_{cr}} = \frac{\tau\omega}{wJ\theta_{cr}} \tag{1}$$

The torque τ was obtained from the relation

$$\tau = I \frac{d\omega}{dt} \tag{2}$$

The determination of the moment of inertia I and the acceleration rate $d\omega/dt$ are discussed subsequently. The static efficiency was obtained from

$$\eta_s = \frac{\Delta h}{\Delta h_{id}} \tag{3}$$

and

$$\Delta h_{id} = C_p T'_0 \left[1 - \left(\frac{p_2}{p'_0} \right)^{(\gamma-1)/\gamma} \right] \tag{4}$$

where p_2/p'_0 is the static- to total-pressure ratio across the turbine.

The moment of inertia I of the rotating assembly was determined experimentally. The assembly was placed on a knife-edge, as shown in figure 9. Small oscillations about the knife-edge were initiated and the period of the oscillations measured. The moment of inertia about the knife-edge was then calculated from the equation for a compound pendulum. Use of the parallel-axis theorem enabled the moment of inertia about the axis of rotation to be determined.

The turbine acceleration rate $d\omega/dt$ was determined from the slope of the turbine-speed-against-time plot. A typical plot is shown in figure 10 and consists of two regions: (1) an accelerating region (region a) in which the turbine is producing work over and above that lost due to bearing friction and windage; and (2) a deceleration region (region b) in which there is no flow through the turbine, the deceleration being caused by the bearing friction and windage losses. If m_a and m_b are the slopes in regions a and b, respectively, then the turbine acceleration rate was calculated by

$$\frac{d\omega}{dt} = m_a - m_b \tag{5}$$

This procedure, in effect, does not penalize the turbine for the windage losses. For certain space applications of interest, the turbine would operate in a hard vacuum and there would be negligible windage losses. Since the unactive portion of the rotor is not

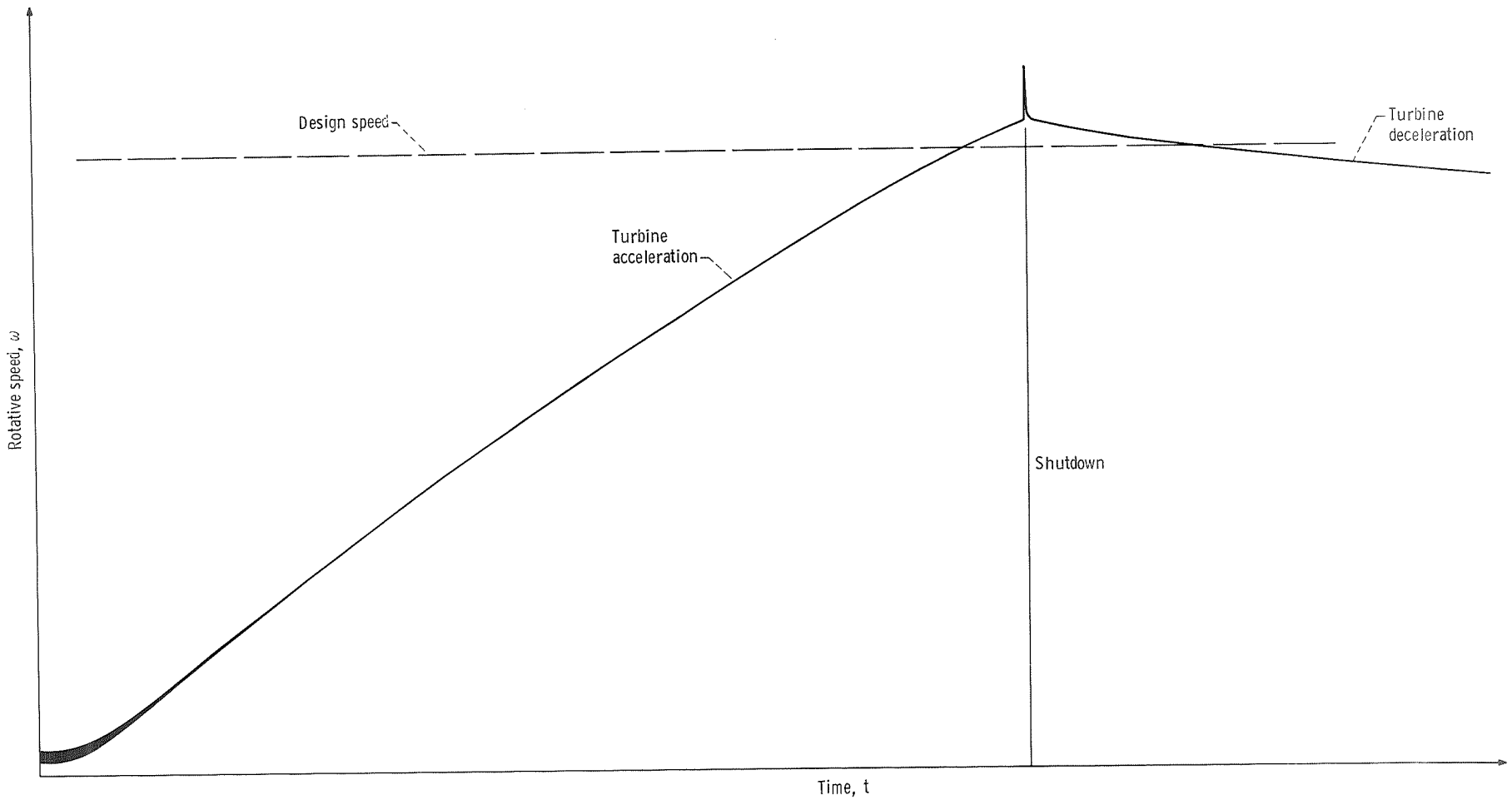

Figure 10. - Typical turbine speed variation during test.

the same on acceleration and deceleration, the windage losses on acceleration and deceleration are not equal. However, because the arc of admission is small, this difference is felt to be small enough to be within the accuracy of the measurements.

RESULTS AND DISCUSSION

Stator Performance

The performance of the stator was measured prior to testing the full turbine. Static-pressure taps were provided along the divergent and straight sections of the nozzle. The instrumented nozzle is shown in figure 11. The nozzles of the full turbine were not instrumented.

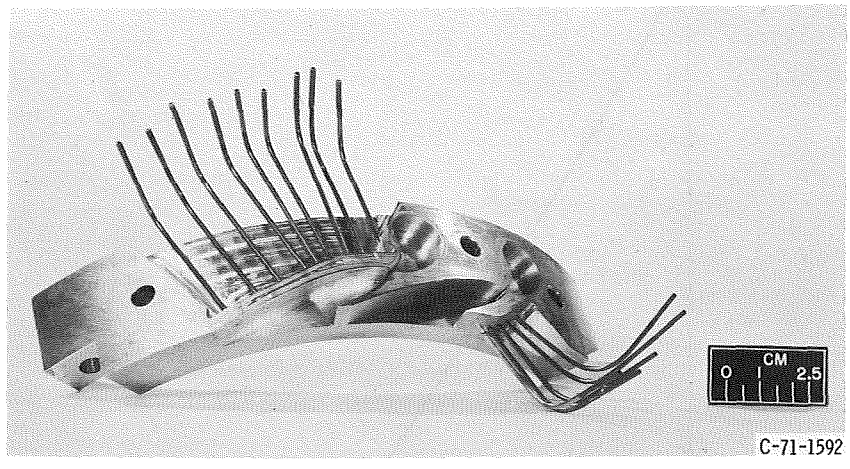

Figure 11. - Instrumented stator.

The pressure variations in the nozzles were obtained at design and off-design conditions and are shown in figure 12. At the design pressure ratio there is good agreement between theory and experiment for the divergent portion of the nozzle. Along the straight section, where the pressure should be theoretically constant, the pressure first decreases below design and then increases. This behavior, which is apparently caused by expansion and shock waves forming on the straight section, would be expected to adversely affect rotor performance if it persisted in the full turbine. At off-design pressure ratios, the pressure increases sharply within the nozzle passage. As is well known, this behavior is typical and is caused by shock wave formation within the nozzle passage.

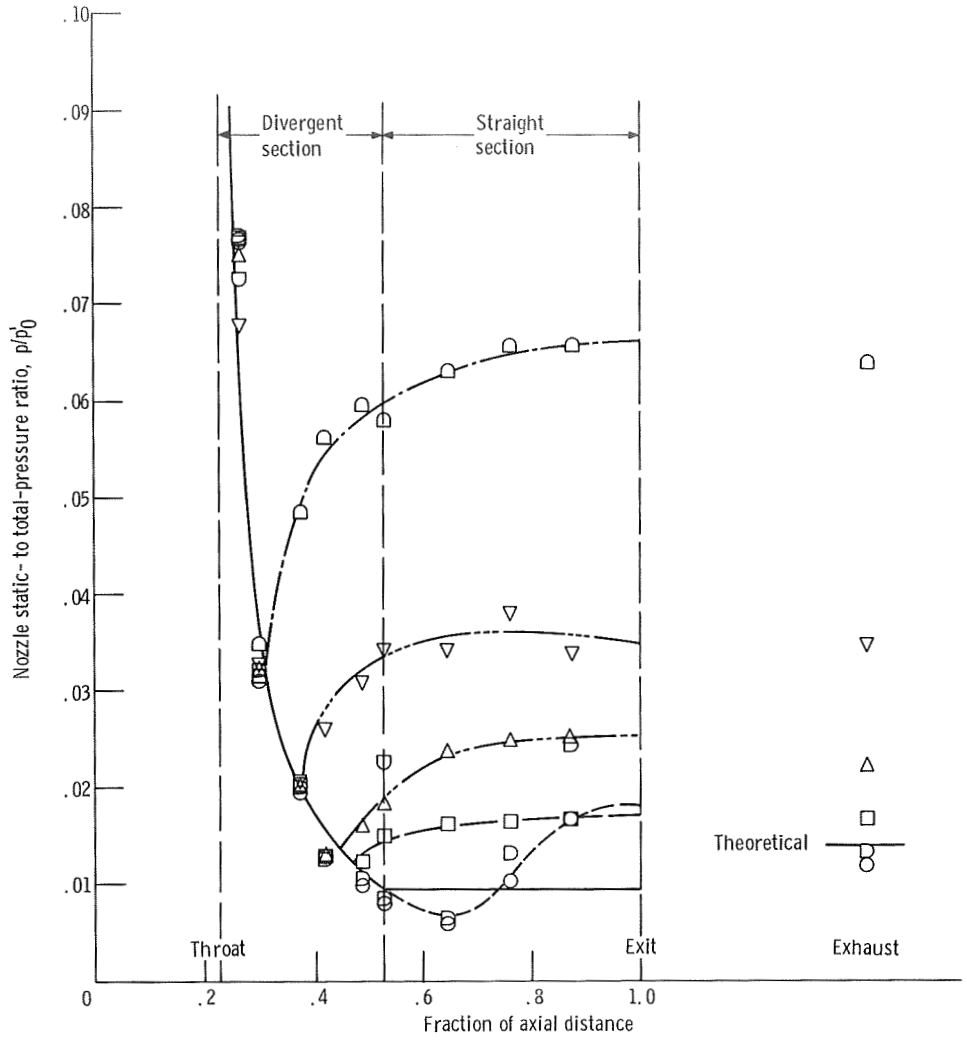

Figure 12. - Variation of nozzle static- to total-pressure ratio with axial distance in nozzle, for constant pressure ratios.

Overall Performance

Weight flow. - The equivalent weight flow for the investigation was about 2.5 percent lower than the design value. This resulted from slight deviations in the stator throat openings from the design value. The flow rate was constant since the stators were choked for all test conditions investigated.

Specific-work and efficiency. - The specific work of the turbine is shown in figure 13 as a function of speed for constant pressure ratios. The static efficiency is shown in figure 14 as a function of blade-jet speed ratio for constant speeds. The total- to static-pressure ratio was varied from 20 to 150 while the speed was varied from 20 to 100 percent of design. For design pressure ratio and equivalent speed the specific work

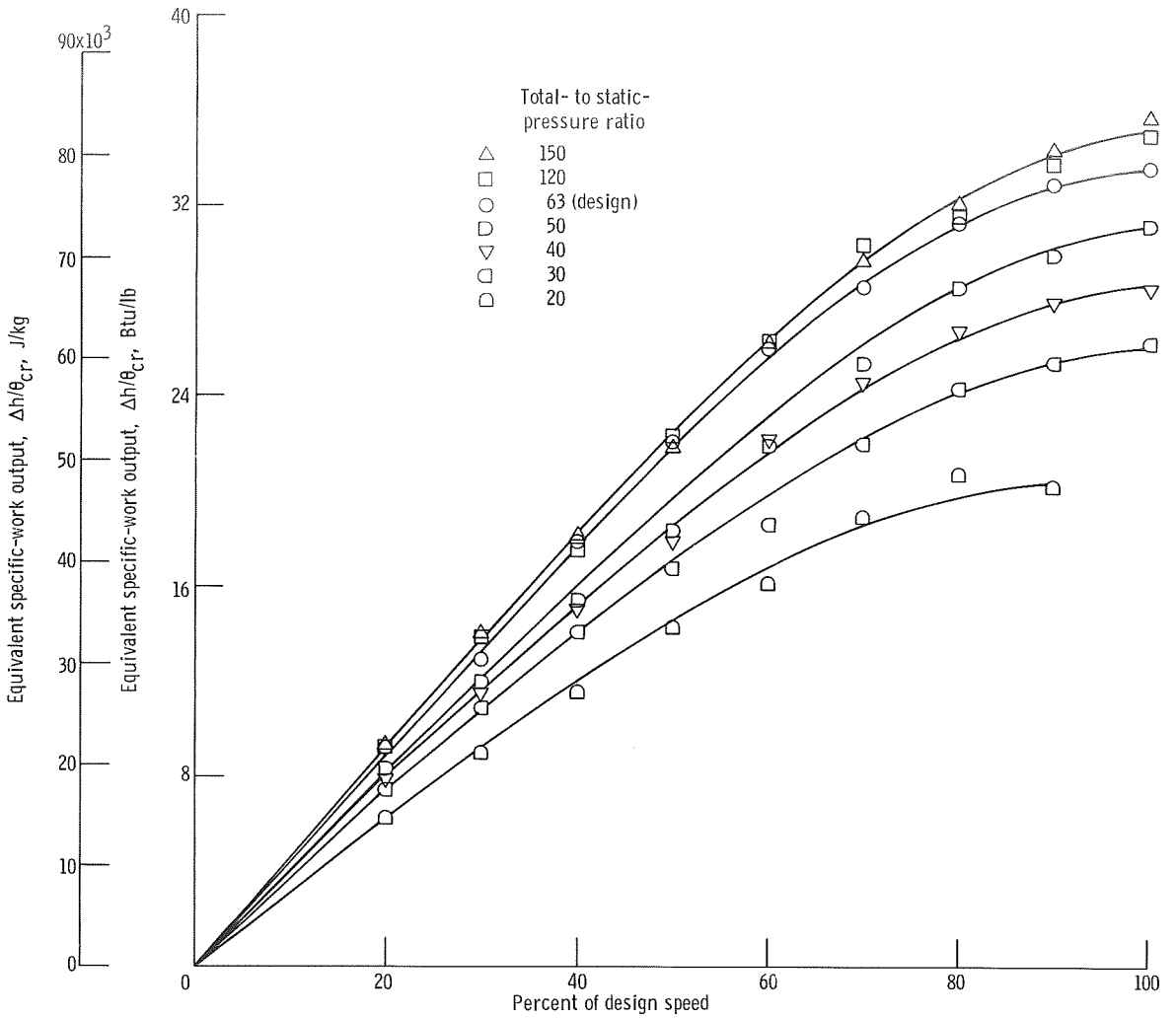

Figure 13. - Equivalent specific-work output of turbine as function of speed, for constant pressure ratios.

obtained was 78.1×10^3 joules per kilogram (33.6 Btu/lb), which is 26 percent lower than the design value. The corresponding static efficiency was 0.390, which is 11 percentage points lower than the design value.

As indicated previously the design procedure was based on boundary layer calculations, which do not take into consideration losses due to shock wave formation (as were found to occur in the nozzle exit section). The boundary layer was also assumed to be turbulent throughout the rotor. A laminar boundary layer would be expected to give higher losses, as would separation of the flow. The efficiency, however, is in reasonable agreement with that obtained from a similar type of turbine (ref. 5). This is discussed further in the next section.

Increasing the pressure ratio above the design value resulted in only a small increase in specific work, indicating that the turbine was operating near limiting loading.

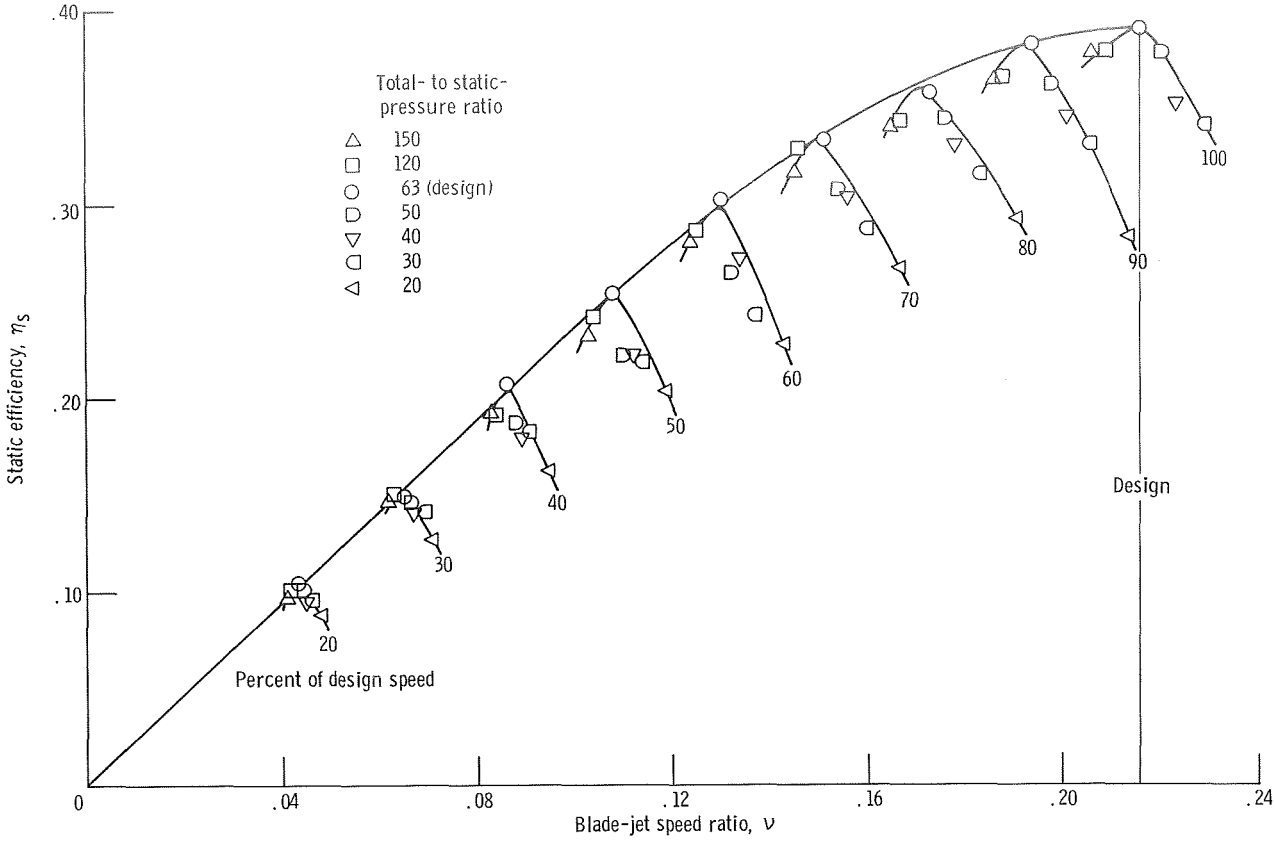

Figure 14. - Static efficiency of turbine as function of blade-jet speed ratio for constant speeds.

The maximum efficiency obtained at any given speed is seen from figure 14 to occur at or near the design pressure ratio. The rapid dropoff of the efficiency at off-design pressure ratios is typical of supersonic turbines and similar to trends found in reference 7.

Comparison with Other Experimental Results

In this section the subject turbine and the turbine described in reference 5 are compared. The single-stage supersonic turbine of reference 5 was designed for a blade-jet speed ratio ν of 0.174 and had a Reynolds number Re, based on blade height, of around 4×10^5. The measured static efficiency η_s obtained at design conditions was 0.414. These values can be compared with the subject turbine values of $\nu = 0.216$, $Re = 75\times10^3$, and $\eta_s = 0.390$. Since decreasing the Reynolds number tends to decrease the efficiency and increasing the blade-jet speed ratio tends to increase the efficiency, a comparison between the two turbines is difficult. However, a comparison can be made using the

performance estimation techniques of reference 8. By using these methods, it is estimated that increasing the Reynolds number of the subject turbine to 4×10^5 would increase the efficiency by approximately 5 percentage points, while decreasing the blade-jet speed ratio would decrease the efficiency by approximately 5 percentage points. It is concluded, therefore, that the subject turbine should have about the same efficiency as the turbine of reference 5, which it does.

SUMMARY OF RESULTS

Turbine performance characteristics were obtained for a single-stage partial-admission supersonic turbine operating at a Reynolds number of approximately 75×10^3. The turbine was tested over a range of pressure ratios from 20 to 150 and equivalent speeds from 20 to 100 percent of design. In addition, the performance of the stator operating alone was obtained. The following results were found:

1. Testing of the stator alone indicated good agreement with theory for the divergent section of the nozzle. On the straight section, however, apparent expansion and shock wave formation resulted in the pressure deviating from the theoretically constant design value.

2. The equivalent turbine specific work at design pressure ratio (63) and equivalent speed was 78.1×10^3 joules per kilogram (33.6 Btu/lb) at a static efficiency of 0.390. These values are considerably lower than those predicted by the boundary layer calculations, which do not take into consideration losses due to shock wave formation (as were found to occur in the nozzle exit section). The performance, however, is in reasonable agreement with previous experimental results.

3. Increasing the turbine pressure ratio above the design value resulted in only a small increase in specific work, indicating that the turbine was operating near limiting loading.

4. The maximum turbine efficiency at any given speed occurred at or near the design pressure ratio and dropped off rapidly at off-design pressure ratios.

Lewis Research Center,
National Aeronautics and Space Administration,
Cleveland, Ohio, June 17, 1971,
120-34.

APPENDIX - SYMBOLS

a speed of sound, m/sec; ft/sec

C_p specific heat at constant pressure, J/(kg)(K); Btu/(lb)(^{o}R)

h specific enthalpy, J/kg; Btu/lb

I moment of inertia about axis of rotation, N-m-sec^2; ft-lb-sec^2

J mechanical equivalent of heat, 778.2 ft-lb/Btu

M Mach number

m slope of speed-against-time curve, rad/sec^2

p absolute pressure, N/m^2; lb/ft^2

R radius of turbine, m; ft

Re Reynolds number, $w_f/\mu R_m$

T temperature, K; ^{o}R

t time, sec

U blade speed, m/sec; ft/sec

V_j velocity corresponding to isentropic expansion from turbine inlet total pressure to turbine exit static pressure, m/sec; ft/sec

w mass-flow rate, kg/sec; lb/sec

γ specific-heat ratio

γ^* specific-heat ratio at U. S. standard air conditions, 1.4

δ ratio of turbine inlet total pressure to U. S. standard sea-level pressure of 10.1325×10^4 N/m^2 (2116.22 lb/ft^2)

ϵ function of γ, $\dfrac{\gamma^*}{\gamma}\left[\dfrac{\left(\frac{\gamma+1}{2}\right)^{\gamma/(\gamma-1)}}{\left(\frac{\gamma^*+1}{2}\right)^{\gamma^*/(\gamma^*-1)}}\right]$

η_s static efficiency

θ_{cr} squared ratio of the critical velocity at turbine inlet to the critical velocity at U. S. standard sea-level air temperature of 288.15 K (518.7^{o} R)

μ viscosity, kg/m-sec; lb/ft-sec

ν blade-jet speed ratio, U_m/V_j

τ torque, N-m; ft-lb

ω rotative speed, rad/sec

Subscripts:

a region of speed-against-time curve where turbine is accelerating

b region of speed-against-time curve where turbine is decelerating

f full admission

id ideal

L lower

m mean

r relative to rotor

U upper

0 stator inlet

1 rotor inlet

2 rotor exit

Superscript:

' total state

REFERENCES

1. Vanco, Michael R.; and Goldman, Louis J.: Computer Program for Design of Two-Dimensional Supersonic Nozzle with Sharp-Edged Throat. NASA TM X-1502, 1968.

2. Goldman, Louis J.; and Scullin, Vincent J.: Analytical Investigation of Supersonic Turbomachinery Blading. I - Computer Program for Blading Design. NASA TN D-4421, 1968.

3. Goldman, Louis J.; and Vanco, Michael R.: Computer Program for Design of Two-Dimensional Sharp-Edged-Throat Supersonic Nozzle with Boundary-Layer Correction. NASA TM X-2343, 1971.

4. Goldman, Louis J.: Analytical Investigation of Blade Efficiency for Two-Dimensional Supersonic Turbine Rotor Blade Sections. NASA TM X-2095, 1970.

5. Moffitt, Thomas P.: Design and Experimental Investigation of a Single-Stage Turbine with a Rotor Entering Relative Mach Number of 2. NACA RM E58F20a, 1958.

6. Moffitt, Thomas P.; and Klag, Frederick W., Jr.: Experimental Investigation of the Partial-Admission Performance Characteristics of a Single-Stage Mach 2 Supersonic Turbine. NASA TM X-80, 1959.

7. Moffitt, Thomas P.; and Klag, Frederick W., Jr.: Experimental Investigation of Partial- and Full-Admission Characteristics of a Two-Stage Velocity-Compounded Turbine. NASA TM X-410, 1960.

8. Stewart, Warner L.: A Study of Axial-Flow Turbine Efficiency Characteristics in Terms of Velocity Diagram Parameters. Paper 61-WA-37, ASME, 1961.

9. Stewart, Warner L.: Analysis of Two-Dimensional Compressible-Flow Loss Characteristics Downstream of Turbomachinery Blade Rows in Terms of Basic Boundary-Layer Characteristics. NACA TN 3515, 1955.

10. Stewart, Warner L.; Whitney, Warren J.; and Wong, Robert Y.: Use of Mean Section Boundary Layer Parameters in Predicting Three-Dimensional Turbine Stator Losses. NACA RME55L12a, 1956.

TABLE I. - STATOR MEAN-SECTION COORDINATES

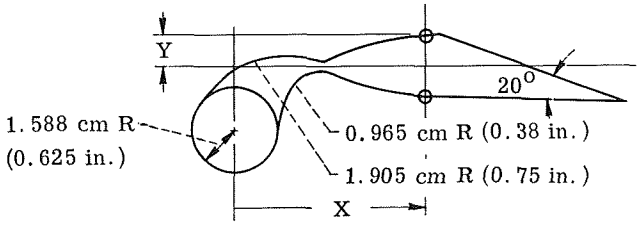

X		Y		X		Y	
cm	in.	cm	in.	cm	in.	cm	in.
1.666	0.656	0.056	0.022	3.503	1.379	0.561	0.221
1.928	.759	.213	.084	3.886	1.530	.582	.229
2.162	.851	.310	.122	4.686	1.845	.594	.234
2.433	.958	.391	.154	5.486	2.160	.605	.238
2.748	1.082	.462	.182	6.287	2.475	.615	.242
3.073	1.210	.513	.202	7.206	2.837	.625	.246

TABLE II. - ROTOR BLADE MEAN-SECTION COORDINATES

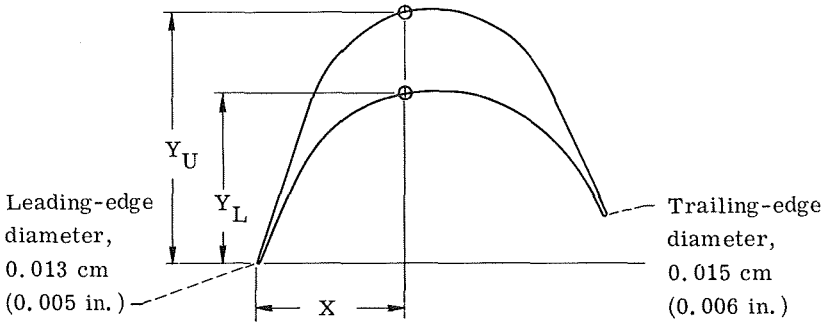

X		Y_L		Y_U		X		Y_L		Y_U	
cm	in.	cm	in.	cm	in.	cm	in.	cm	in.	cm	in.
0.012	0.005	0.004	0.002	0.045	0.018	0.711	0.280	0.616	0.243	0.920	0.362
.041	.016	.078	.031	.129	.051	.772	.304	.608	.239	.909	.358
.071	.028	.157	.062	.223	.088	.833	.328	.589	.232	.888	.350
.102	.040	.229	.090	.312	.123	.894	.352	.570	.224	.854	.336
.132	.052	.292	.115	.404	.159	.955	.376	.540	.213	.807	.318
.163	.064	.346	.136	.495	.195	1.016	.400	.498	.196	.742	.292
.193	.076	.395	.155	.587	.231	1.047	.412	.474	.187	.695	.274
.224	.088	.431	.170	.661	.260	1.077	.424	.445	.175	.637	.251
.254	.100	.465	.183	.717	.282	1.108	.436	.413	.163	.572	.225
.285	.112	.489	.193	.757	.298	1.138	.448	.376	.148	.504	.199
.346	.136	.532	.209	.817	.322	1.169	.460	.335	.132	.438	.172
.407	.160	.564	.222	.860	.338	1.199	.472	.290	.114	.372	.146
.468	.184	.588	.232	.890	.350	1.230	.484	.242	.095	.306	.121
.529	.208	.604	.238	.912	.359	1.260	.496	.193	.076	.242	.095
.590	.232	.615	.242	.923	.363	1.284	.506	.151	.059	.190	.075
.650	.256	.620	.244	.925	.364						

NASA-Langley, 1971 — 1 E-6380

NATIONAL AERONAUTICS AND SPACE ADMISTRATION
WASHINGTON, D.C. 20546

OFFICIAL BUSINESS
PENALTY FOR PRIVATE USE $300

FIRST CLASS MAIL

POSTAGE AND FEES PAID
NATIONAL AERONAUTICS AND
SPACE ADMINISTRATION

U.S.MAIL

POSTMASTER: If Undeliverable (Section 158 Postal Manual) Do Not Return

"The aeronautical and space activities of the United States shall be conducted so as to contribute . . . to the expansion of human knowledge of phenomena in the atmosphere and space. The Administration shall provide for the widest practicable and appropriate dissemination of information concerning its activities and the results thereof."

—NATIONAL AERONAUTICS AND SPACE ACT OF 1958

NASA SCIENTIFIC AND TECHNICAL PUBLICATIONS

TECHNICAL REPORTS: Scientific and technical information considered important, complete, and a lasting contribution to existing knowledge.

TECHNICAL NOTES: Information less broad in scope but nevertheless of importance as a contribution to existing knowledge.

TECHNICAL MEMORANDUMS: Information receiving limited distribution because of preliminary data, security classification, or other reasons.

CONTRACTOR REPORTS: Scientific and technical information generated under a NASA contract or grant and considered an important contribution to existing knowledge.

TECHNICAL TRANSLATIONS: Information published in a foreign language considered to merit NASA distribution in English.

SPECIAL PUBLICATIONS: Information derived from or of value to NASA activities. Publications include conference proceedings, monographs, data compilations, handbooks, sourcebooks, and special bibliographies.

TECHNOLOGY UTILIZATION PUBLICATIONS: Information on technology used by NASA that may be of particular interest in commercial and other non-aerospace applications. Publications include Tech Briefs, Technology Utilization Reports and Technology Surveys.

Details on the availability of these publications may be obtained from:

SCIENTIFIC AND TECHNICAL INFORMATION OFFICE

NATIONAL AERONAUTICS AND SPACE ADMINISTRATION

Washington, D.C. 20546